



AMS
American Meteorological Society

Supplemental Material

© [Copyright 2023 American Meteorological Society](#) (AMS)

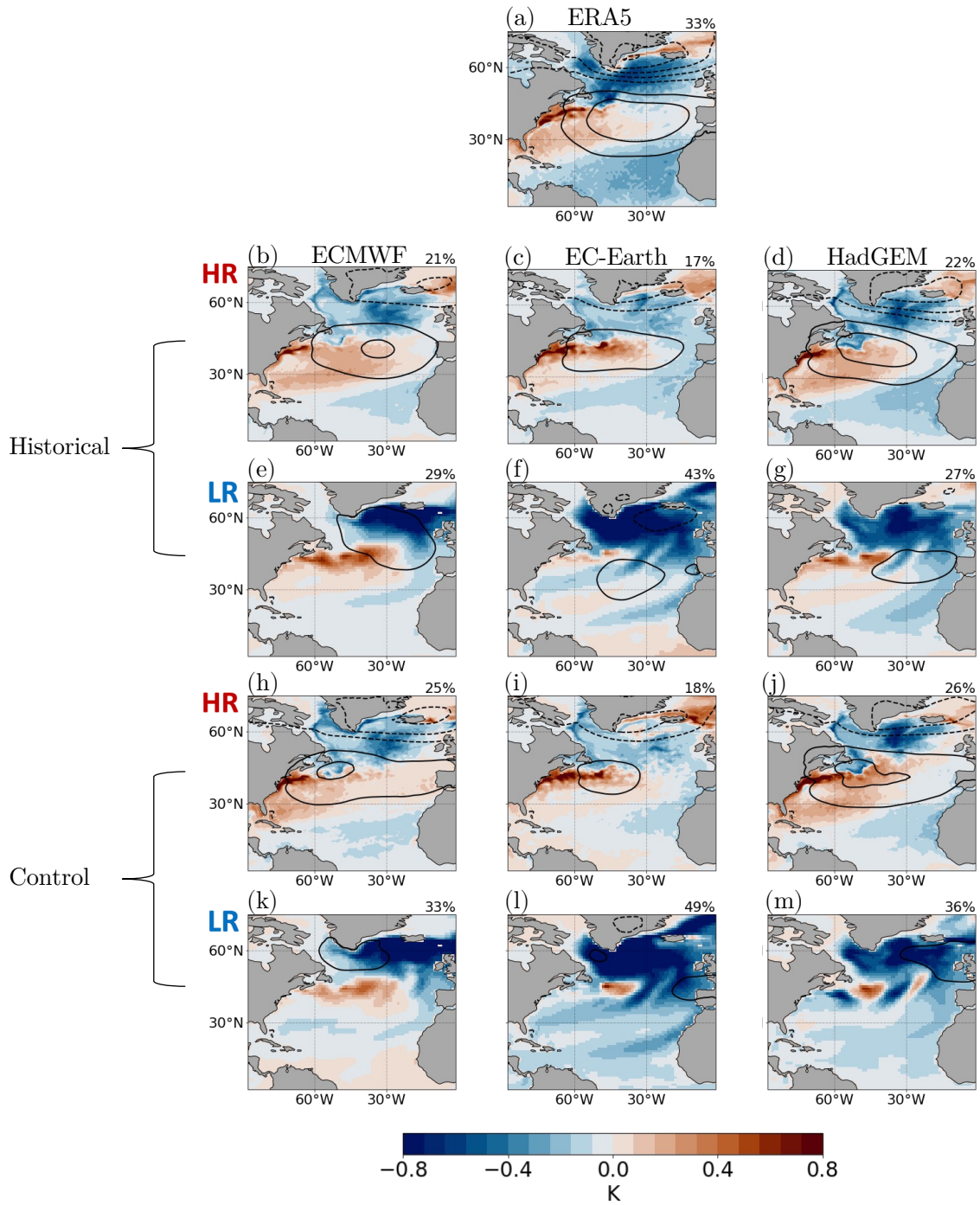
For permission to reuse any portion of this work, please contact permissions@ametsoc.org. Any use of material in this work that is determined to be “fair use” under Section 107 of the U.S. Copyright Act (17 USC §107) or that satisfies the conditions specified in Section 108 of the U.S. Copyright Act (17 USC §108) does not require AMS’s permission. Republication, systematic reproduction, posting in electronic form, such as on a website or in a searchable database, or other uses of this material, except as exempted by the above statement, requires written permission or a license from AMS. All AMS journals and monograph publications are registered with the Copyright Clearance Center (<https://www.copyright.com>). Additional details are provided in the AMS Copyright Policy statement, available on the AMS website (<https://www.ametsoc.org/PUBSCopyrightPolicy>).

1 **Supplementary Material for “Improved Extratropical North Atlantic**
2 **Atmosphere–Ocean Variability with Increasing Model Resolution”**

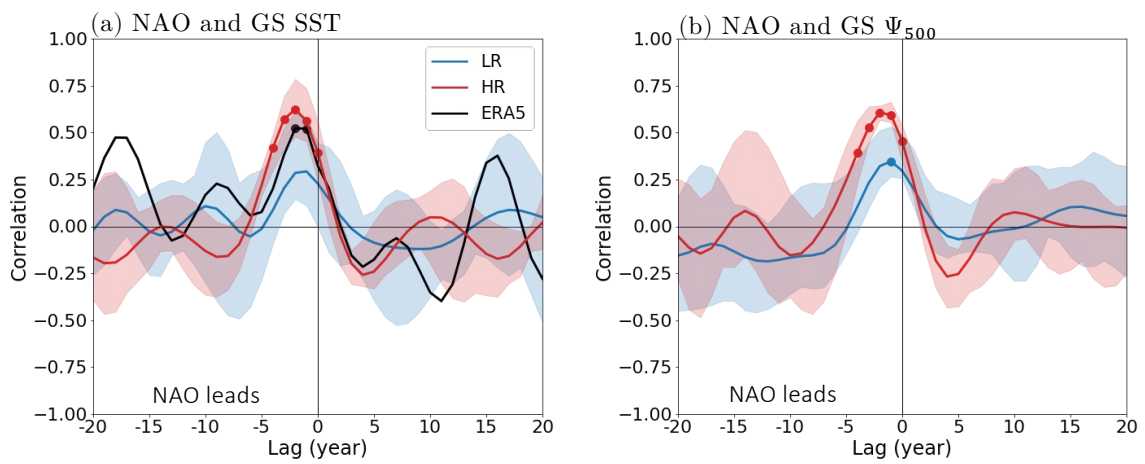
3 Casey R. Patrizio^a, Panos J. Athanasiadis^a, Claude Frankignoul^{b,c}, Doroteaciro Iovino^a,
4 Simona Masina^a, Luca Famooss Paolini^a and Silvio Gualdi^a.

5 ^a *Centro Euro-Mediterraneo sui Cambiamenti Climatici (CMCC), Bologna, Italy.*

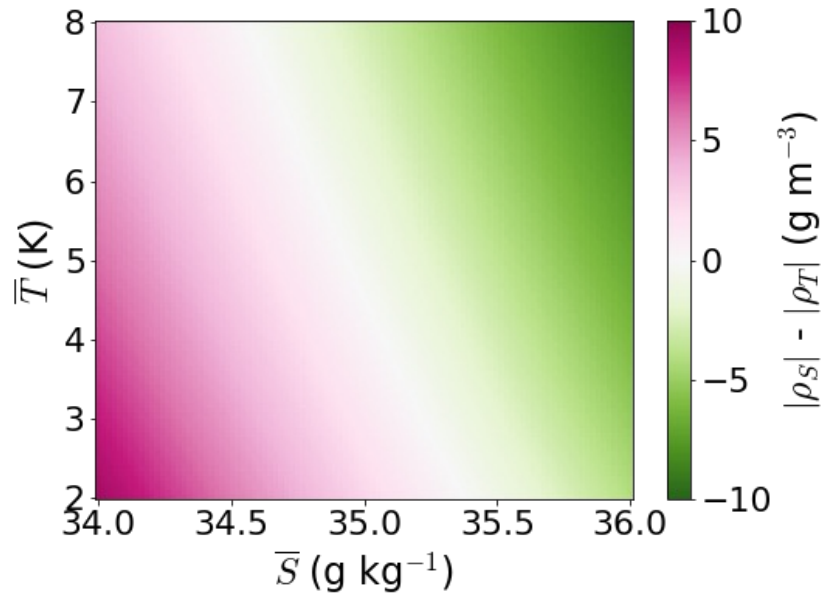
6 ^b *Sorbonne University, Paris, France.* ^c *Woods Hole Oceanographic Institution, USA*



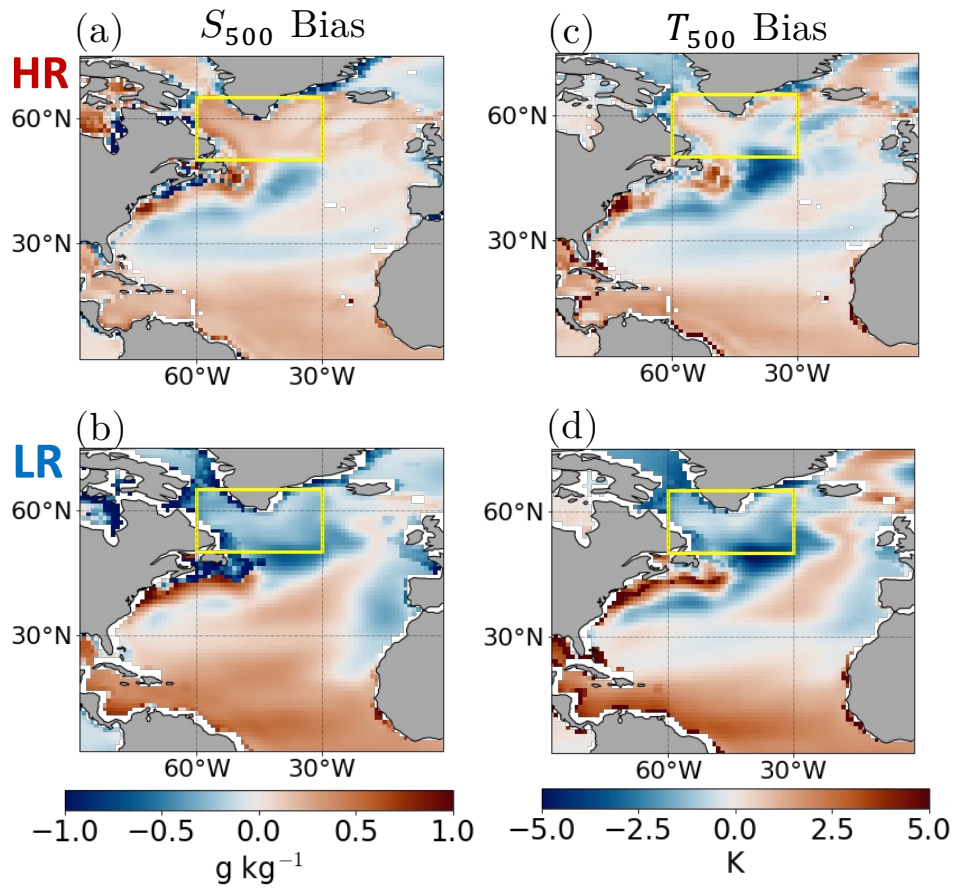
9 FIG. S1. (a–g) As in Figure 1a–g of the main text, except a 7-year low-pass filter as been applied to the fields
 10 before calculating the leading EOF of SST and the SLP regression pattern. (h–m) As in (a–g), except for the
 11 control runs from ECMWF, EC-Earth and HadGEM.



12 FIG. S2. The cross-correlation between low-pass filtered (a) NAO and SST anomalies averaged over the Gulf
 13 Stream region ($37\text{--}47^\circ\text{N}$, $30\text{--}70^\circ\text{W}$), and (b) NAO and Ψ_{500} anomalies averaged over the Gulf Stream region.
 14 Multi-model ensemble-mean correlations are calculated from the LR model runs (blue lines) and HR model runs
 15 (red lines) with the associated spread across the model runs indicated by transparent shading. The black line in
 16 (a) shows results for ERA5.



17 FIG. S3. The impact of mean temperature (vertical axis; K) and mean salinity (horizontal axis; g kg^{-1}) on
 18 density anomalies (shading; g m^{-3}). A perturbation of $\delta T = 0.8\text{K}$ is applied to equation of state for range of
 19 mean S and T to produce density perturbation ρ_T . A perturbation of $\delta S = 0.38 \text{ g kg}^{-1}$ is applied to the equation
 20 of state for the same range of mean S and T to produce density perturbation ρ_S . Note that the perturbation values
 21 and range of mean T and S are chosen to approximate typical conditions in the subpolar region. The difference
 22 between the magnitudes of ρ_S and ρ_T is shown. Pink shading indicates that the magnitude of ρ_S exceeds the
 23 magnitude of ρ_T and green shading indicates vice versa.



24 FIG. S4. Multi-model mean bias in upper-ocean salinity (S_{500} ; g kg^{-1}) for the (a) HR control runs and (b)
 25 LR control runs from ECMWF, EC-Earth and HadGEM. (c, d) As in (a, b), except for upper-ocean temperature
 26 (T_{500} ; K). The biases are calculated relative to observed S_{500} and T_{500} from EN4 data. The yellow box indicates
 27 the Labrador-Irminger sea region discussed in the main text.

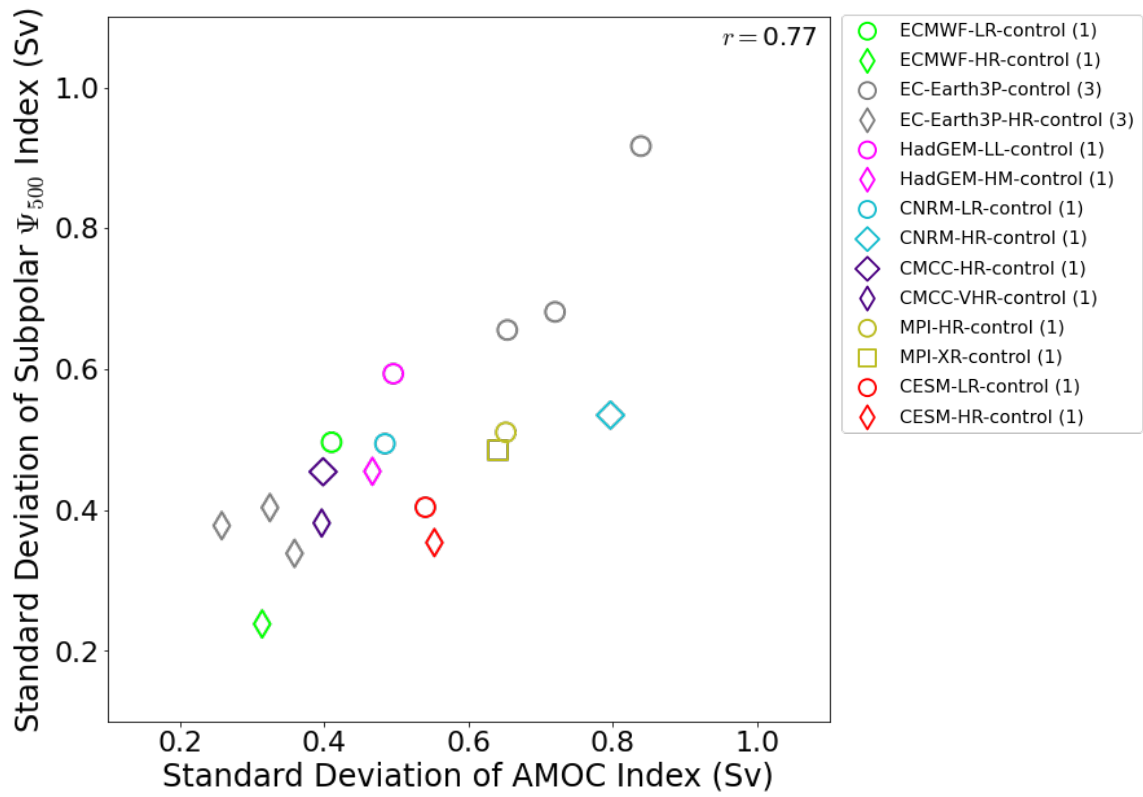
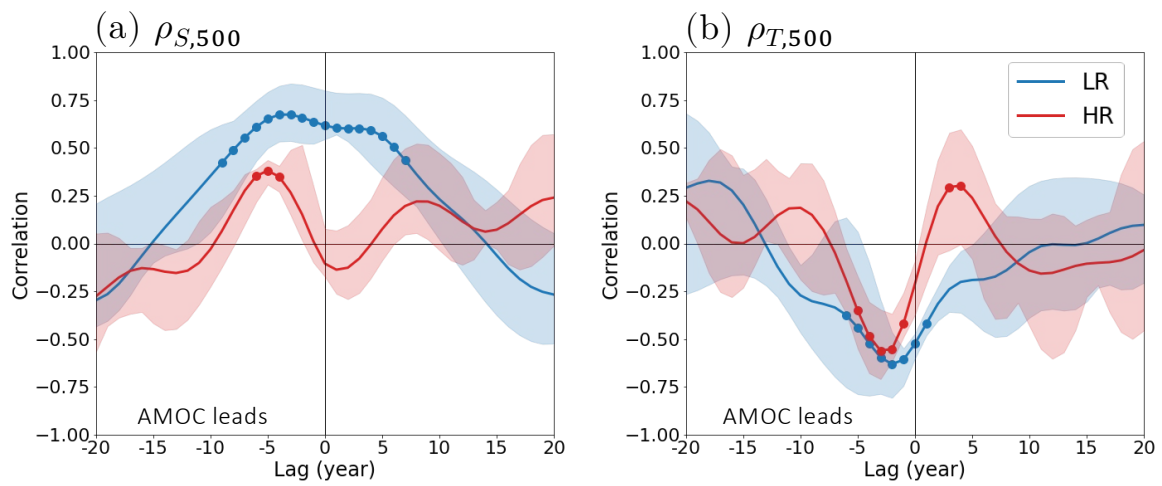


FIG. S5. As in Figure 10b of the main text, except markers have been colored by the model name.



28 FIG. S6. As in Figure 11 of the main text, except for the cross-correlation between (a) the AMOC index
 29 and the salinity component of subpolar ρ_{500} anomalies ($\rho_{S,500}$), and (b) the AMOC index and the temperature
 30 component of subpolar ρ_{500} anomalies ($\rho_{T,500}$).